Physica A 563 (2021) 125466

Contents lists available at ScienceDirect

Physica A

journal homepage: www.elsevier.com/locate/physa

Robustness of supply chain networks against underload cascading failures

Qihui Yang *, Caterina M. Scoglio, Don M. Gruenbacher

Department of Electrical and Computer Engineering, Kansas State University, Manhattan, KS, 66506, USA

A R T I C L E I N F O

Article history:
Received 26 December 2019
Received in revised form 17 September 2020
Available online 20 October 2020

Keywords:
Cascading failure
Robustness
Supply chain
Complex network

A B S T R A C T

In today's global economy, supply chain (SC) entities have become increasingly interconnected with demand and supply relationships due to the need for strategic outsourcing. Such interdependence among firms not only increases efficiency but also creates more vulnerabilities in the system. Natural and human-made disasters such as floods and transport accidents may halt operations and lead to economic losses. Due to the interdependence among firms, the adverse effects of any disruption can be amplified and spread throughout the systems. This paper aims at studying the robustness of SC networks against cascading failures. Considering the upper and lower bound load constraints, i.e., inventory and cost, we examine the fraction of failed entities under load decrease and load fluctuation scenarios. The simulation results obtained from synthetic networks and a European supply chain network (Cardoso et al., 2015) both confirm that the recovery strategies of surplus inventory and backup suppliers often adopted in actual SCs can enhance the system robustness, compared with the system without the recovery process. In addition, the system is relatively robust against load fluctuations but is more fragile to demand shocks. For the underload-driven model without the recovery process, we found an occurrence of a discontinuous phase transition. Differently from other systems studied under overload cascading failures, this system is more robust for power-law distributions than uniform distributions of the lower bound parameter for the studied scenarios.

1. Introduction

Cascading failures and network robustness have been studied extensively in real-world networks such as power systems and traffic networks [1–8]. Failures in these models are often overload-driven. Pahwa et al. [8] built a simple but realistic overload cascade model for power systems and studied its emergent behavior against power outages, which can lead to the load redistribution across the network and result in more failures due to the power flows exceeding the line capacity. They observed a sudden breakdown of the system with an increased load level and a large network size. Many works study the cascading failure phenomenon from a single network perspective, and there have also been recent studies of failure cascades in interdependent networks. Buldyrev et al. developed in [9] a one-to-one correspondence model to study the robustness of interconnected networks against cascading failures, and found that removal of a critical fraction of nodes could lead to a complete breakdown of the system. Since the work [9], many works have studied the

* Corresponding author.
E-mail address: qihui@ksu.edu (Q. Yang).

https://doi.org/10.1016/j.physa.2020.125466

robustness of interdependent networks from various perspectives [10–17], in which disruptions of components in one system may propagate and cause elements in the other system to fail.

In the competitive economic market, SC entities often build business relationships with outsourcing partners to reduce the overall cost and promote productivity. As a result, SCs have become more complicated and geographically dispersed, increasing the frequencies of SC disruptions [18]. Due to the increased dependencies among entities, disruptions of a company's operation can result in revenue losses in its business partners, and cascade to other components in the SC [19]. On the other hand, sustainability concerns have pushed for higher efficiency in the use of resources and reduction in protective redundancies in SCs, thus making SCs more susceptible to disruptions [20]. SC entities may suffer from financial losses due to delays in the flow of goods caused by natural disasters or intentional attacks. For example, heavily relying upon transportation services for timely delivery of animals among ranches, stockers, feedlots, and meat-processing plants, the beef industry can suffer substantial economic losses due to disruptions in transportation infrastructure caused by natural disasters and movement restrictions during disease outbreaks [11]. During the 2011 Japan earthquake and tsunami, Toyota Motor Company suffered at least a 140,000-vehicle production loss. This adverse effect spread to other countries, which led to a massive collapse in the global automotive and electronics industry [21]. In the following weeks after the disaster, Toyota in North America experienced shortages of over 150 parts, resulting in curtailed operations at only 30% of capacity [22].

In light of these low probability and high impact disruptions, several studies have utilized the above overload failure models to analyze the SC robustness against cascading failure [23–25]. From a complex network perspective, a supply chain is also termed a supply network, in which network nodes and links refer to the SC entities and supply–demand relationships between the entities, respectively. Cluster SC network is a typical SC network based on industry clusters. Zeng and Xiao studied the dynamic robustness of cluster SC networks under overloaded cascading failures, and found that network load entropy can help identify the cascading failure phenomenon with large damage at its early stage, thereby avoiding the collapse of the whole network [23]. Tang et al. [24] examined the robustness of an interdependent SC network model, which consists of an undirected cyber layer and a directed physical layer, subject to different node removal strategies. However, the nature of cascading failures in SC systems is mostly underload-driven. When entities cannot fulfill the expected production requirement to overcome the fixed production costs, they will fail to gain profit and possibly exit the market. When a node is disrupted, its downstream and upstream neighbors will be affected due to supply shortage and demand losses, respectively. If the neighboring node's remaining load drops below the lower bound constraint, i.e., cost, new failure occurs, and cascades to other nodes in the entire system [26,27]. Tang et al. [28] assessed the SC system robustness in the form of production capability losses, but they assumed that the failed node loads only propagate downstream without consideration of mitigation strategies. Wang et al. [26] attempted to improve the cluster SC network resilience against cascading failures, leveraging insights from the ant colony's spatial fidelity zones. In the model developed by Wang et al. a node can propagate the failure impact both upstream and downstream, and can dynamically change the strength of the business relationship with its neighbors [27]. Sun et al. proposed a multi-echelon supply chain evolutionary model and performed robustness analyses under different attack strategies. They assumed that node failures are caused by insufficient load, and successive failures happen only among nodes that have certain symbiotic relationships [29]. Huo et al. proposed a two-layer network to study the SC risk propagation under warning information diffusion. In their work, a risk propagation threshold is derived and found to have correlations with the network topology, the herd mentality, and the risk reference [30]. There also exists a series of studies focusing on the design of optimal recovery methods to cope with disturbance or disruptions in SC networks [31,32]. To the best of the authors' knowledge, there are few works considering underload-driven failures, and this work attempts to add a new element to this domain with a focus on the phase transition behavior.

Given the tremendous damages caused by the disruptions, understanding the nature of the systemic failure in SC that goes beyond a single component behavior is a significant problem to be addressed. The goal of this work is to build an underload cascade failure model and analyze its behavior against disruptive events. First, we will build a generalized underload cascade failure model with and without recovery strategies. The material flow of goods through an entity node defines its load. Second, we will examine the fraction of failed nodes in the system under scenarios of load decrease and load fluctuations. Third, we will provide analytic results based on the assumption of equal load redistribution upon failures for the studied scenarios.

The contributions of this paper are: (i) Using the proposed model with recovery strategies, we confirm that strategies of backup suppliers and surplus inventories, often adopted in actual SCs, improve the system robustness. In addition, the system is relatively robust against load fluctuations but is more fragile to load decrease. (ii) Without the recovery process, we found numerically and analytically a discontinuous phase transition of the system under a load decrease scenario. Based on statistical physics, this indicates that a small fraction of failures can result in a sudden breakdown in the SC system. More specifically, the model is more robust under the power-law distribution than the uniform distribution of the lower bound load parameter for the studied scenarios. These findings indicate that underload driven systems have different behaviors against cascading failures compared with overload cascade models, and need to be further explored.

2. Underload cascading failure model

2.1. Load and load constraints

In multi-hierarchy SC networks, nodes are entities and edges denote the supply–demand relationships between the entities. SC entities are both demand-side and supply-side, and those in the same tier have similar network connections, core businesses, and competitive environments [33–35].

In this work, we represent the SC as follows:

$$G = (V, E, L, A, B) \tag{1}$$

where $V = \{v_1, v_2, \ldots, v_n\}$ is a set of nodes, and $E = \{(v_i, v_j)|e_{ij} = 1 \text{ or } 0\}$ is a set of edges. When $e_{ij} = 1$, there is a directed link between nodes v_i and v_j; otherwise, $e_{ij} = 0$.

$L = \{L_1, L_2, \ldots, L_n\}$ is a set of node loads. We define the load of a node $L_i(t)$ as the sum of material flows that go through an entity node, i.e., the total number of products that an entity has sold per time unit. $A = \{A_1, A_2, \ldots, A_n\}$ and $B = \{B_1, B_2, \ldots, B_n\}$ are sets of node load constraints. More specifically, A_i denotes the upper bound load for node i, which is the maximum number of products an entity can provide, i.e., inventory. B_i denotes the lower bound load for node i, and reflects costs such as labor costs and maintenance fees.

Suppose the SC network has T number of tiers, and the initial loads for nodes in the last tier T, equivalent to the demand for final customers, are known and equal. To initialize the node load and load constraints in the network, we first calculate weights on all edges, which reflect the business relationship strength between node entities. Weight on edge e_{ij} is calculated by $w_{ij} = (d_i \cdot d_j)^{\theta}$, with $\theta = 0.5$ [26,27]. d_i denotes the node degree of node i, and is obtained by $d_i = d_i^{+} + d_i^{-}$, where d_i^{+} and d_i^{-} are the indegree and outdegree of node i, respectively.

Given initial node loads in tier T, we calculate all initial flows on edges between nodes in tier T-1 and tier T as follows:

$$F_{i,j}(0) = L_j(0) \cdot w_{ij} / \sum_{k \in \Gamma_j^U} w_{kj} \tag{2}$$

where $F_{i,j}(t)$ is the flow on edge e_{ij} at time t and $w_{ij}/\sum_{k \in \Gamma_j^U} w_{kj}$ indicates the fraction of the supplies from supplier i with respec to all suppliers of node j. Γ_j^U is the node collection consisting of upstream nodes connected to node j.

According to the node load definition, the initial load of each node in tier T-1 equals the sum of its outgoing flows, which is given by

$$L_i(0) = \sum_{j \epsilon \Gamma_i^D} F_{i,j}(0) \tag{3}$$

where Γ_i^D is the node collection consisting of downstream nodes connected to node i.

After obtaining the initial loads of nodes in tier T-1, we calculate the initial node loads in tier T-2 using Eqs. (2)–(3). Similarly, we sequentially calculate the initial loads of nodes in all tiers backward, i.e., T-3, …, 2, 1. As a result, the sum of incoming flows equals the sum of outgoing flows for each node i, i.e., $L_i(t) = \sum_{m \epsilon \Gamma_i^U(t)} F_{m,i}(t) = \sum_{j \epsilon \Gamma_i^D(t)} F_{i,j}(t)$, with demand and supply balanced, which is in accordance with the node load definition.

In terms of node load constraints, we assume that A_i and B_i are proportional to the initial node load $L_i(0)$, and are given as follows

$$\begin{cases} A_i = aL_i(0) \\ B_i = bL_i(0) \end{cases} \tag{4}$$

where a is the upper bound parameter, $a > 1$; b is the lower bound parameter, $0 < b < 1$.

2.2. Cascading failure process

In the normal state, the network is in the steady state and the load of node i at time t satisfies $B_i < L_i(t) < A_i$. When an SC network suffers from disruptive events, some nodes can be underloaded and fail initially. Caused by the connections between the entities, the impact of these initial failures could result in more failures and spread to the entire system. In this work, we consider the cascading failure processes with and without recovery measures as follows.

Step 1: We initialize the node load $L_i(0)$ for each node i in the network, and then calculate load constraints (A_i and B_i) based on the value of $L_i(0)$. Keeping the load constraints for each node unchanged, we decrease or fluctuate the initial node loads to simulate initial failures. The new initial load of node i after the load decrease or fluctuations is denoted as $L_i'(0)$.

Step 2: Caused by the new failures, node load loss propagates throughout the system, and all the loads and flows affected are updated.

Step 3: With recovery measures, the nodes affected but not yet failed can reduce load losses by altering flows with existing partners or by building new partners.

Then, if there are still nodes with loads below their lower bound load, i.e., $L_i(t) < B_i$, these nodes will be marked as failed and we continue the process from Step 2–3. Such a procedure is repeated until no new failure happens. Failure of a node indicates that the entity receives insufficient load and fails to gain profit in the competitive market.

2.2.1. Node load loss propagation scheme

We assume that if a node fails, it can neither receive supplies from upstream neighbors, nor ship products to downstream partners. Thus, once a node i fails at time t, both its load and the flows on its incoming and outgoing edges are set to zero. Here we use $\Delta_i^-(t)$ to denote the load loss of node i at time t, and $\Delta_{m,i}^-(t)$ to denote the load loss of node m influenced by node i at time t. $F_{i,j}(t)$ denotes the flow from node i to node j at time t.

We model the impact of the failed node i on its upstream nodes as follows. For node i failed at time t, its upstream neighboring node m in Γ_i^U will suffer load loss $\Delta_{m,i}^-(t)$. Accordingly, the load of node m, i.e., $L_m(t)$, and the flow $F_{m,i}(t)$ on edge e_{mi} are updated according to Eq. (5). Furthermore, the affected node m will lead to the load loss of node d in its upstream neighboring set, Γ_m^U.

$$\begin{cases} \Delta_i^-(t) = L_i(t-1) = \sum_{p\in\Gamma_i^U} F_{p,i}(t-1) \\ \Delta_{m,i}^-(t) = \Delta_i^-(t)F_{m,i}(t-1)/\sum_{p\in\Gamma_i^U} F_{p,i}(t-1) = F_{m,i}(t-1) \\ L_m(t) = L_m(t-1) - \Delta_{m,i}^-(t) \\ F_{m,i}(t) = F_{m,i}(t-1) - \Delta_{m,i}^-(t) = 0 \\ \Delta_{d,m}^-(t) = \Delta_{m,i}^-(t)\,F_{d,m}(t-1)\,/\sum_{q\in\Gamma_m^U} F_{q,m}(t-1) \\ L_d(t) = L_d(t-1) - \Delta_{d,m}^-(t) \\ F_{d,m}(t) = F_{d,m}(t-1) - \Delta_{d,m}^-(t) \end{cases} \tag{5}$$

where $m\in\Gamma_i^U$ and $d\in\Gamma_m^U$. Summation $\sum_{p\in\Gamma_i^U} F_{p,i}(t-1)$ is the sum of flows on the incoming edges of node i, and $F_{m,i}(t-1)/\sum_{p\in\Gamma_i^U} F_{p,i}(t-1)$ indicates the fraction of the newly load loss allocated to node m with respect to the total load loss of node i.

In addition, the load loss of node i is propagated to downstream nodes. Due to the failure of node i, its downstream neighboring node s reduces load by $\Delta_{s,i}^-(t)$. The flow between nodes i and s is also updated. As the load loss propagates further downstream, we also decrease the load of node r, which is the downstream neighboring of node s, and the corresponding flow $F_{s,r}(t)$ according to Eq. (6).

$$\begin{cases} \Delta_i^-(t) = L_i(t-1) = \sum_{g\in\Gamma_i^D} F_{i,g}(t-1) \\ \Delta_{s,i}^-(t) = \Delta_i^-(t)F_{i,s}(t-1)\,/\sum_{g\in\Gamma_i^D} F_{i,g}(t-1) = F_{i,s}(t-1) \\ L_s(t) = L_s(t-1) - \Delta_{s,i}^-(t) \\ F_{i,s}(t) = F_{i,s}(t-1) - \Delta_{s,i}^-(t) = 0 \\ \Delta_{r,s}^-(t) = \Delta_{s,i}^-(t)\,F_{s,r}(t-1)\,/\sum_{h\in\Gamma_s^D} F_{s,h}(t-1) \\ L_r(t) = L_r(t-1) - \Delta_{r,s}^-(t) \\ F_{s,r}(t) = F_{s,r}(t-1) - \Delta_{r,s}^-(t) \end{cases} \tag{6}$$

where $s\in\Gamma_i^D$ and $r\in\Gamma_s^D$.

The node load loss propagation process continues upstream to tier 1 and downstream to tier T, mimicking the ripple effect spreading throughout the system.

To clearly illustrate the load loss propagation after nodes failed, we present a simplified example on a four-tier SC network, as shown in Fig. 1. Assuming that nodes 9 and 13 fail at time t, the load they lose will affect their neighboring nodes 4, 14, 15 and 8, 18 through connectivity links. Then, affected nodes 14, 15 further impact their downstream nodes 18, 19 and 20 by reducing supply. Meanwhile, node 8 influences its upstream neighboring nodes

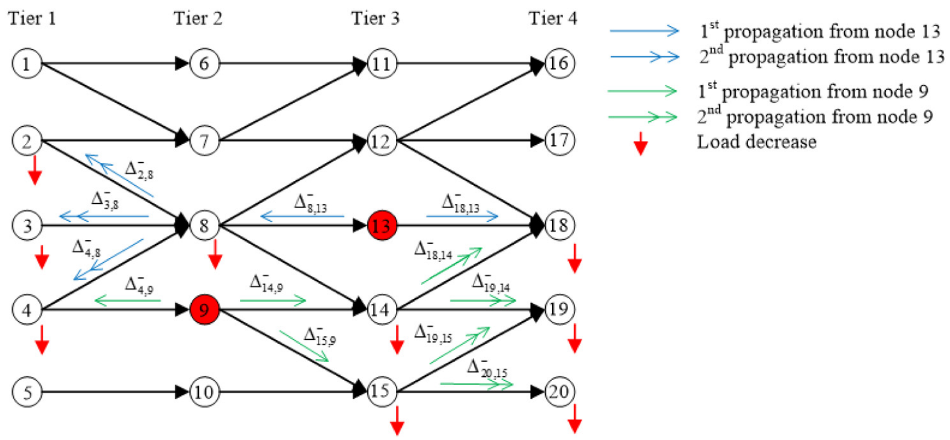

Fig. 1. An example of load loss propagation in a four-tier supply chain. Red circles represent the initial failures caused by load decrease or fluctuations.

2, 3 and 4 by cutting back demand. It is worth noting that the load loss suffered by node 4 is affected by nodes 8 and 9 at the same time, thus its load at time t is decreased by $\Delta^-_{4,8}(t) + \Delta^-_{4,9}(t)$, where $\Delta^-_{4,9}(t) = L_9(t-1)$ and $\Delta^-_{4,8}(t) = \Delta^-_{8,13}(t) F_{4,8}(t-1) / \sum_{q \epsilon \Gamma^U_8} F_{q,8}(t-1)$.

2.2.2. Load loss recovery scheme

In this section, the load loss recovery scheme is designed to simulate that entities can mitigate their losses by requesting rush orders or building new business partnerships during disruptive events. We define the residual load of node i at time t as $RL_i(t) = A_i - L_i(t)$, which indicates the additional available products an entity can provide, i.e., surplus inventory. Each node can at most provide its residual load when it helps its neighbor to recover losses.

When recovery measures are considered in the cascading failure model, only surviving nodes can recover their node load when suffering from load losses. Note that after the load loss propagation process, a node with $L_i(t) < B_i$ can recover its load if it is not marked as failed. If the node's load, $L_i(t)$, is still below its lower bound load, B_i, after the recovery process, this node will be marked as failed, and cause further load losses in the next step.

Since acquiring new partners will bring additional costs, we assume node i (not yet permanently failed) will first select from surviving nodes in its upstream neighboring set, Γ^U_i, and downstream neighboring set, Γ^D_i, to recover load losses. If all the neighboring nodes' residual load still cannot help it recover above B_i, node i will build links with surviving nodes in its upstream non-neighboring set, $\overline{\Gamma}^U_i(t)$, and downstream non-neighboring set, $\overline{\Gamma}^D_i(t)$.

According to the node load definition, each node's demand and supply are balanced in the steady state. Therefore, the impact of the increase in a node load will spread upstream to tier 1 and downstream to tier T. Then, it is easy to understand that the total load increase of nodes in each tier s, $\sum_{i \epsilon \Omega_s} \Delta^+_i$ should always be equal, where Ω_s is the node collection consisting of surviving nodes in tier s and s = 1, 2, …, T. In this section, we use $\Delta^+_i(t)$ to denote the load increase of node i, and $\Delta^+_{m,i}(t)$ to denote the load increase of node m influenced by node i.

Note that as the numbers of surviving nodes in each tier at time t are not necessarily the same, the total load loss for each tier, i.e., $\sum_{i \epsilon \Omega_s}(L'_i(0) - L_i(t))$, are different. In addition, the total residual loads for each tier, i.e., $\sum_{i \epsilon \Omega_s} RL_i(t)$, are also different.

The load loss recovery process is described as follows:

Due to the aforementioned reasons, we identify the tier γ_a with the minimum residual load, RL_{MIN}, and tier γ_b with the maximum loss, ΔL_{MAX} (Eq. (7)). The total load increase of each tier, $\sum_{i \in tiers} \Delta^+_i(t)$, equals the smaller value of RL_{MIN} and ΔL_{MAX}.

$$\begin{cases} RL_{MIN} = \min\limits_{s} \left[\sum\limits_{i \epsilon \Omega_s} RL_i(t) \right], s = 1, 2, \ldots, T \text{ and } \gamma_a = s^* \\ \Delta L_{MAX} = \max\limits_{s} \left[\sum\limits_{i \epsilon \Omega_s} (L'_i(0) - L_i(t)) \right], s = 1, 2, \ldots, T \text{ and } \gamma_b = s^* \\ \sum\limits_{i \epsilon \Omega_s} \Delta^+_i = \min(RL_{MIN}, \Delta L_{MAX}), s = 1, 2, \ldots, T \end{cases} \tag{7}$$

If $RL_{MIN} < \Delta L_{MAX}$, we first recover nodes in tier $\gamma = \gamma_a$ with the load of each node i increased by $\Delta^+_i(t) = RL_i(t)$, $i \epsilon \Omega_{\gamma_a}$. Otherwise, if $RL_{MIN} \geq \Delta L_{MAX}$, we first recover node load in tier $\gamma = \gamma_b$, and each node load increases by $\Delta^+_i(t) = L'_i(0) - L_i(t)$, $i \epsilon \Omega_{\gamma_b}$.

Similar to the load propagation process, the impact of load increase in tier γ will spread upstream and downstream to the entire system. Suppose node i is in tier γ, and its load gets increased by $\Delta_i^+(t)$. To imitate that node i requests a rush order from its supplier m, we increase $F_{m,i}(t)$ and the load of node m by $\Delta_{m,i}^+ = \min(\Delta_i^+(t), RL_m(t))$, $m \epsilon \Gamma_i^U = \Omega_{\gamma-1}$. If the first randomly selected supplier m's residual load cannot satisfy the order request of node i ($RL_m(t) < \Delta_i^+(t)$), node i will continue to randomly select the next supplier in Γ_i^U. If all suppliers still fail to meet the request of node i, i.e., $\sum_{m\in\Gamma_i^U} RL_m(t) < \Delta_i^+(t)$, node i will build links with randomly selected nodes in the non-neighboring set $\overline{\Gamma}_i^U(t)$, until objective $\Delta_i^+(t) = \sum_{m\epsilon\Gamma_i^{U'}} \Delta_{m,i}^+$ is met, where $\Gamma_i^{U'}$ is the new node collection consisting of all upstream neighboring nodes connected to node i .

Load increase of node m will further lead to load increase of its upstream nodes. This process continues until all related suppliers in tier 1 have increased their loads. Similarly, loads of surviving nodes downstream are updated.

3. Numerical simulation results

Researchers often study the phase transition behavior exhibited by the system through stressing external forces to it until the rupture point [36]. In this section, we examine the robustness of the SC networks under the stress of load decrease and fluctuations. Note that each node's load constraints, A_i and B_i, remained fixed as strength of the stress δ or σ changes under each scenario.

As the failures are underload-driven, we conduct extensive simulations with lower bound parameter b following (i) uniform and (ii) power-law distribution, which are two commonly used families of distributions [8,37]. Uniformly distributed over $[b_{min}, b_{max}]$, denoted by U$[b_{min}, b_{max}]$, the probability density function for a random variable b is given by $p(b) = 1/(b_{max} - b_{min}) \cdot 1_{b_{min}\le b\le b_{max}}$. Following a power-law distribution, the probability density function for a random variable b is of the form $p(b) = k \cdot (b)^{-\gamma}$ with $b \in [b_{min}, 1]$.

3.1. Synthetic networks

Hernández and Pedroza-Gutiérrez [38] constructed random network models in bipartite graphs to model the theoretical SC networks. Similarly, we generate synthetic networks for a four-tier SC network, as shown in Fig. 1, representing suppliers, production centers, distribution centers, and customers. N nodes are generated and equally divided into four tiers, in which one enterprise node belongs only to one tier. Links are created randomly with a given connection probability p, which is the likelihood of existing business relationships between nodes in two tiers. Additional efforts are made to ensure the network created is without self-loops. Despite the random placement of links, most nodes will have approximately the same number of connections. For example, the average node outdegree of a network with 100 nodes in each tier ($N = 400$) and $p = 0.1$ will be around 10.

3.1.1. Load decrease

In this scenario, we consider a negative demand shock, in which demand for goods or services shrinkages suddenly. To model the load decrease, we simultaneously decrease the initial loads for all nodes in tier 4 by a factor δ, i.e., $L_i'(0) = (1-\delta) L_i(0)$, and then calculate all the flows and node loads in tiers 1–3. Keeping the network topology unchanged, it is equivalent to a uniform decrease of all the nodes by a factor δ. In each realization, δ changes from 0 to 1 with a step size of 0.02. We record the fraction of failed nodes f at the end of the simulation, and the results are averaged over 100 realizations with network size $N = 400$ and connection probability $p = 0.1$.

In Fig. 2(a)–(c), we found a sharp collapse of the system when there are no recovery measures and b is uniformly distributed over $[b_{min}, b_{max}]$. More specifically, the critical point above which the failure occurs is only determined by b_{max}, the upper limit of the uniform distribution. For example, in Fig. 2(b), in which B_i ranges between $[0.2L_i(0), 0.7L_i(0)]$, when $\delta > 0.3$, i.e., $L_i'(0) < 0.7L_i(0)$, initial failures start to appear and will propagate throughout the system, resulting in the collapse of the whole system.

When recovery measures are included and $b \in$ U$[b_{min}, b_{max}]$, results in Fig. 2(a)–(c) show that the recovery strategy can reduce the scale of systemic failure, as the reconfiguration of the trade flows among alive nodes can absorb losses of nodes affected by the initial failures. In Fig. 2(b), when $\delta > 0.8$, i.e., $L_i'(0) < 0.2L_i(0)$, all the loads fail at the beginning and are marked as failed, so they will not mitigate losses under the recovery process.

With b in the form of power distribution, the system collapses when δ increases to 0.88 without recovery process in Fig. 2(d), indicating that the system becomes more robust compared to the uniform distribution case.

3.1.2. Load fluctuations

We mimic the load fluctuations by setting final customers' new initial load as $L_i'(0) = (1+\sigma\xi_i) L_i(0)$, i.e., $L_i'(0) \in [(1-\sigma) L_i(0), (1+\sigma) L_i(0)]$, where ξ_i is a random variable uniformly distributed in $[-1, 1]$. Then, we calculate the new initial loads for the nodes in tier 1–3 and flows on the edges. It is equivalent to allowing all the initial loads to fluctuate by a fraction of σ. When σ varies between [0, 1], upper bound parameter a is set to be two to ensure $L_i'(0) < A_i$, with $A_i = aL_i(0)$. Results are averaged over 100 runs of the simulation, with network size $N = 400$ and connection probability $p = 0.1$.

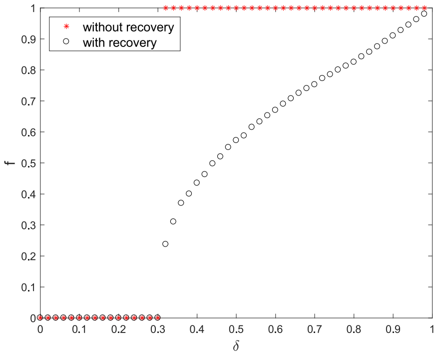

(a) $b \in$ U[0, 0.7]

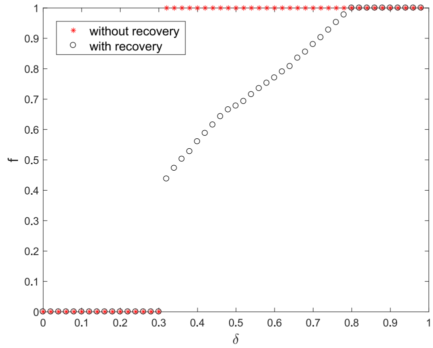

(b) $b \in$ U[0.2, 0.7]

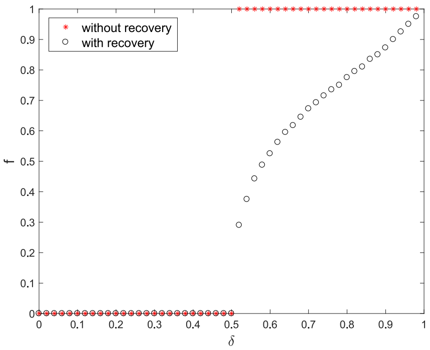

(c) $b \in$ U[0, 0.5]

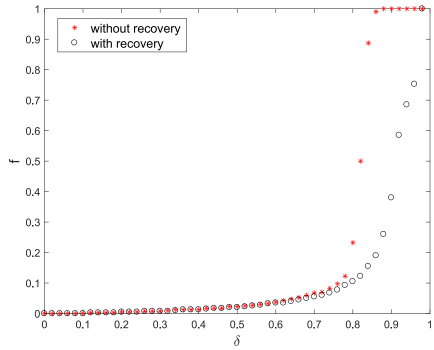

(d) $p(b) \propto b^{-2}$ with $b \in [0.02, 1]$

Fig. 2. Plots of the fraction of failed nodes f versus the relative load decrease δ mimicking the demand shock.

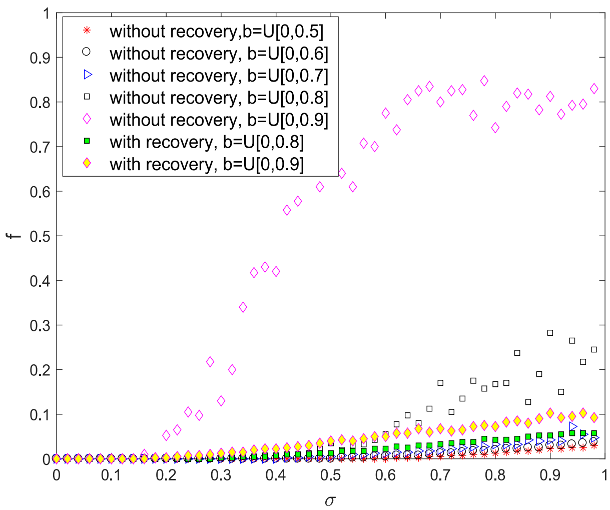

Fig. 3. Plot of the fraction of failed nodes f versus the relative strength of load fluctuations σ.

Fig. 3 shows the changes in the fraction of failed nodes as variation size σ increases. Compared with the load decrease scenario, the system collapse happens less abruptly. When recovery measures are not included and b is uniformly distributed over [0, 0.9], the fraction of failed nodes reaches a plateau of around 80% as fluctuation escalates. In comparison, when b is uniformly distributed over [0, 0.8], about 25% of nodes failed in the end, suggesting that the system is relatively robust.

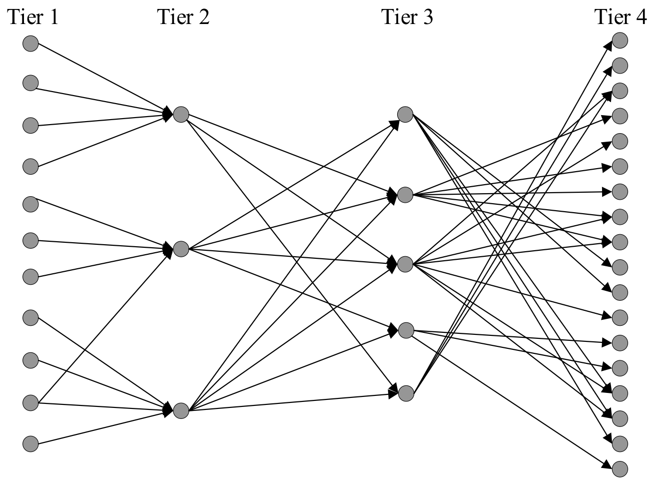

Fig. 4. Network structure of a European supply chain.
Source: From Cardoso et al. [39].

3.2. Real-world example

The underload cascading model proposed in this work is independent of the network topologies and can be applied to other types of SC networks. In this section, we apply the proposed model to a European supply chain network obtained from [39], which includes 11 raw materials suppliers, 3 plants, 5 warehouses, and 18 markets (Fig. 4).

As shown in Fig. 5, simulation results under load decrease/fluctuation scenarios coincide with previous simulation results obtained from synthetic networks. Regarding load decrease, we observe a discontinuous phase transition for the system without recovery measures, and this system becomes more robust with the addition of recovery measures. Also, the system is relatively robust in the case of load fluctuations. For instance, without recovery measures, the fraction of failed nodes varies between 40%–50% when the relative strength of load fluctuations σ is larger than 0.66.

4. Mean-field analysis

In this section, we forecast a discontinuous transition for the cascading failure model without the recovery process using mean-field analysis. In power systems, power flows can redistribute in the whole system upon failures according to the Kirchhoff's law, which is dependent on power line impedance. Similarly, the effects of disruptions can spread to the entire SC network, and the flow redistribution in the system is dependent on the business relationships among entities. This feature inspires us to leverage the equal load redistribution model that has been used in power systems [8,37,40,41]. The assumption is that when a node fails, the load it carries before the failure will be redistributed equally among all the remaining nodes. The equal load redistribution assumption is originated from the widely used democratic fiber bundle model [42], in which N parallel fibers with different failure capacity share an applied force equally.

In the following, we analyze the load decrease scenario using a simple equal-load redistribution model. Suppose there are N nodes with a lower bound load B_i characterized by a probability distribution $p(B)$, and failures happen in discrete time steps $t = 0, 1\ldots$ The fraction of failed nodes and the number of surviving nodes until cascade stage t is denoted as f_t and N_t respectively. When the load of a node goes below B_i, the node fails and its load gets redistributed equally among the remaining surviving nodes.

Suppose all the nodes initially carried the same load $\bar{L}_0'$. There is no failure before the disruptions, thus $f_0 = 0$ and $N_0 = N$. Under disruptions, a fraction of nodes $f_1 = \int_{\bar{L}_0'}^{\infty} p(B)\, dB$ immediately fails, since their load $\bar{L}_0'$ is below the lower bound load. After the first stage, the number of surviving nodes equals to $N_1 = (1 - f_1)\, N$, and the new load per node becomes $\bar{L}_1 = \bar{L}_0' - \frac{f_1 \bar{L}_0' N}{(1-f_1)N} = \left(1 - \frac{f_1}{1-f_1}\right)\bar{L}_0'$. The cascade failure process continues recursively, and the mean-field equations for the $(t+1)$th stage are as follows:

$$\begin{cases} f_{t+1} = \int_{\bar{L}_t}^{\infty} p(B)\, dB \\ N_{t+1} = (1 - f_{t+1})\, N \\ \bar{L}_{t+1} = \bar{L}_t - (f_{t+1}N - f_t N)\, \bar{L}_t / N_{t+1} = [1 - (f_{t+1} - f_t)/(1 - f_{t+1})]\bar{L}_t \end{cases} \tag{8}$$

where $(f_{t+1}N - f_t N)/N_{t+1}$ is $\frac{\text{Number of lines that survive stage } t \text{ but fail at } t+1}{\text{Number of lines that survive stage } t+1}$.

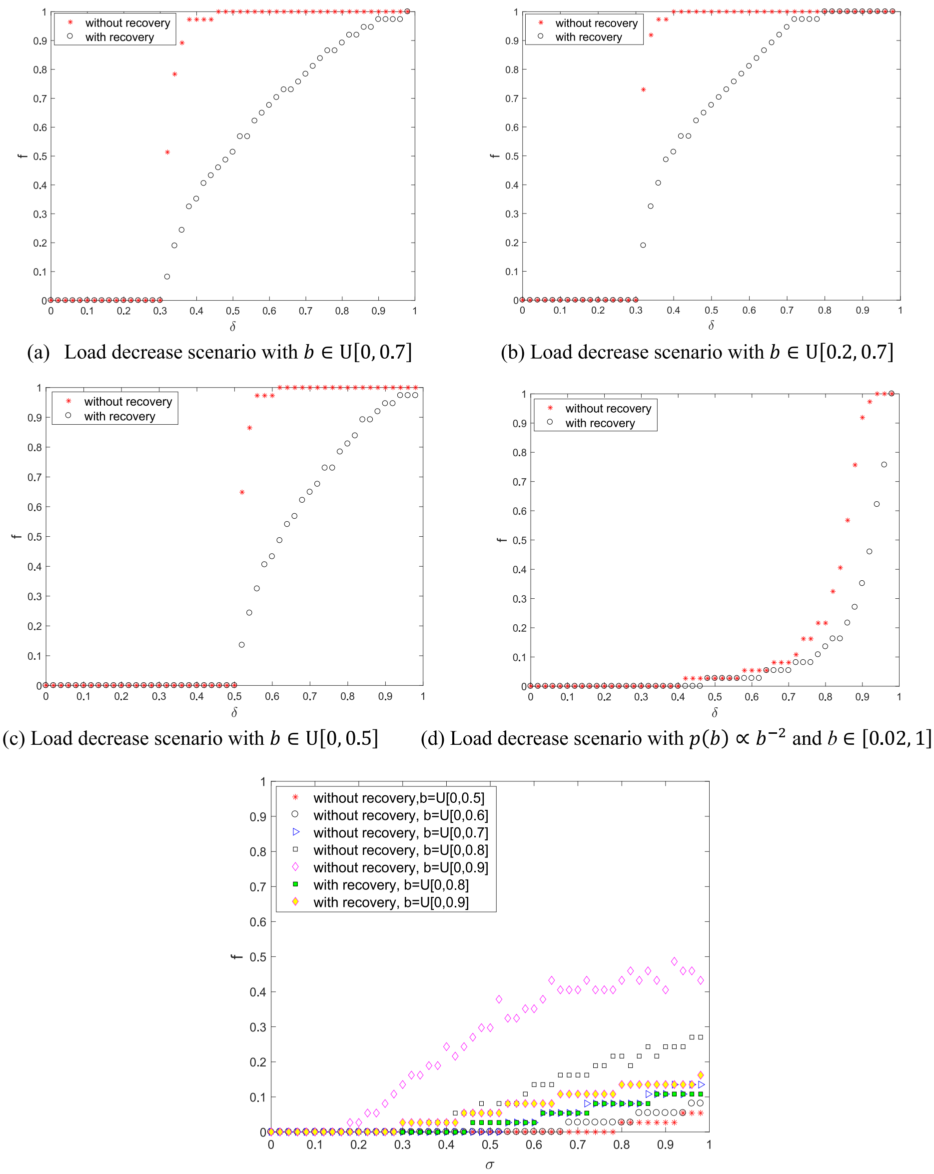

(a) Load decrease scenario with $b \in U[0, 0.7]$ (b) Load decrease scenario with $b \in U[0.2, 0.7]$

(c) Load decrease scenario with $b \in U[0, 0.5]$ (d) Load decrease scenario with $p(b) \propto b^{-2}$ and $b \in [0.02, 1]$

(e) Load fluctuation scenario

Fig. 5. Simulation results using the European supply chain network.

Eq. (8) can be simplified as

$$f_{t+1} = F(\overline{L}_0' \prod_{t=1}^{t} (1 - \frac{f_t - f_{t-1}}{1 - f_t})) \tag{9}$$

where $F(x) = \int_x^{\infty} p(B)\, dB$.

From Eq. (9), we can see that the critical point f^* is mainly dependent on the distribution of B_i. To obtain the fraction of failed nodes, we provide analytic solutions by numerically solving Eq. (9) and verify them by simulating the above equal-load redistribution process under disruptions. We assume the initial node load $\overline{L}_0 = 1$ before the disruptions, and thus lower bound load $B_i = b\overline{L}_0 = b \cdot 1$ with $b \in [b_{min}, b_{max}]$. Under load decrease, the new initial load becomes $\overline{L}_0' = (1 - \delta)\, \overline{L}_0 = (1 - \delta) \cdot 1$.

The results obtained from the simulation are averaged over 100 runs and compared with the results calculated from equations in Fig. 6, in which a discontinuous phase transition occurs in all cases. In the uniform distribution case, the critical point below which a sudden collapse happens is only determined by b_{max}. When the new initial load $\overline{L}_0'$ is above

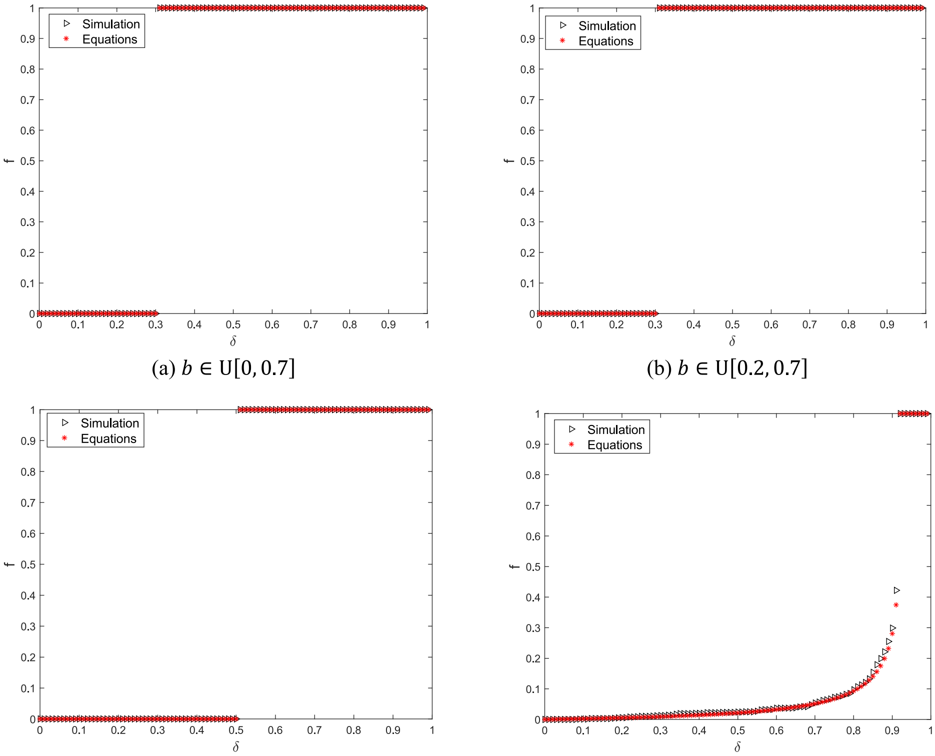

(a) $b \in \mathrm{U}[0, 0.7]$

(b) $b \in \mathrm{U}[0.2, 0.7]$

(c) $b \in \mathrm{U}[0, 0.5]$

d) $p(b) \propto (b)^{-2}$ with $b \in [0.02, 1]$

Fig. 6. Plots of the fraction of failed nodes f as a function of the relative load decrease δ using the mean-field model.

B_i, there are no failures in the system. Once $\overline{L}_0'$ falls below B_i, the system collapses because the fraction of failed node obtained from the equation will increase to 1. When b follows a power-law distribution, the system is more robust, and there is an abrupt breakdown of the system at $\delta \approx 0.9$. Interestingly, this is contrary of the mean-field result for the overload cascade model [8], in which the discontinuous jump happens with no precursors in power-law distributions, and with precursors in line capacity following a uniform distribution. This indicates that the scale of cascade failures in SCs could be significantly affected by the shape of the b distribution, which is closely related to a company's cost.

5. Conclusions

In this paper, we constructed an underload cascading failure model to study the robustness of SC networks under load decrease and load fluctuation scenarios. Most real-world SCs are equipped with redundancies such as surplus inventory and backup suppliers, and our simulation results from both synthetic networks and real network topologies show that the recovery strategies can significantly reduce the scale of the systemic failure when disruptive events happen. In addition, the system is relatively robust under the load fluctuation scenario, as the fraction of failed nodes escalates only when variation size σ is very high without considering recovery measures, which rarely happens in reality. Compared to the load fluctuations, the system appears more vulnerable against disruptive events such as load decrease, i.e., demand shock, and SC decision-makers need to take proactive protection measures to reduce or avoid the impact of such disruptive events.

Since many cascading failure models do not consider the recovery process, we also studied the behavior of the proposed underload-driven model without the recovery measures. We found that the model exhibits a discontinuous phase transition behavior under load decrease scenario as predicted by the mean-field analysis. More specifically, under different distributions of lower bound parameter b, i.e., cost per output, the system is more robust when b follows a power distribution compared to the uniform distribution for the studied scenarios. These emergent behaviors observed are different from the analytic results derived from the overload-driven system by Pahwa et al. [8], in which the power-law distribution of capacity results in a more abrupt system breakdown.

In this paper, we qualitatively show the dynamic behavior of specific SC networks against disruptions and do not take the whole complexity of SCs into account. For example, the proposed model disregards the possible internal connections between entities in the same tier. Future work can add more features to the current model and analyze the system behavior under disruptive events. Since the links in the SC synthetic network are randomly generated based on a connection probability and we disrupt all nodes with a factor δ or σ, the initial failures triggered in this work can be seen as caused by random attacks. More simulations can be conducted to examine the phase transition behavior of SC systems under targeted attacks with various network topologies. In this work, we mainly focus on the robustness assessment, thus designing an optimal recovery strategy is not our primary focus. The recovery process developed assumes that SC entities have full knowledge of the surplus inventory information in the whole system, and future work can include more realistic assumptions regarding mitigation strategies.

CRediT authorship contribution statement

Qihui Yang: Conceptualization, Methodology, Formal analysis, Software, Validation, Writing - original draft. **Caterina M. Scoglio:** Conceptualization, Methodology, Validation, Funding acquisition, Writing - review & editing. **Don M. Gruenbacher:** Conceptualization, Methodology, Funding acquisition, Validation, Writing - review & editing.

Declaration of competing interest

The authors declare that they have no known competing financial interests or personal relationships that could have appeared to influence the work reported in this paper.

Acknowledgments

This work was supported by the National Science Foundation, USA under Grant Award CMMI-1744812. The contents of the paper do not necessarily reflect the position or the policy of funding parties.

References

[1] Y. Koç, M. Warnier, P. Van Mieghem, R.E. Kooij, F.M.T. Brazier, A topological investigation of phase transitions of cascading failures in power grids, Physica A 415 (2014) 273–284, http://dx.doi.org/10.1016/j.physa.2014.07.083.
[2] Y. Koç, M. Warnier, P.V. Mieghem, R.E. Kooij, F.M.T. Brazier, The impact of the topology on cascading failures in a power grid model, Physica A 402 (2014) 169–179, http://dx.doi.org/10.1016/j.physa.2014.01.056.
[3] Y. Hou, X. Xing, M. Li, A. Zeng, Y. Wang, Overload cascading failure on complex networks with heterogeneous load redistribution, Physica A 481 (2017) 160–166, http://dx.doi.org/10.1016/j.physa.2017.04.039.
[4] F. Xue, E. Bompard, T. Huang, L. Jiang, S. Lu, H. Zhu, Interrelation of structure and operational states in cascading failure of overloading lines in power grids, Physica A 482 (2017) 728–740, http://dx.doi.org/10.1016/j.physa.2017.04.061.
[5] J.J. Wu, H.J. Sun, Z.Y. Gao, Cascading failures on weighted urban traffic equilibrium networks, Physica A 386 (2007) 407–413, http://dx.doi.org/10.1016/j.physa.2007.08.034.
[6] L. Zhang, J. Lu, B. Fu, S. Li, A cascading failures model of weighted bus transit route network under route failure perspective considering link prediction effect, Physica A 523 (2019) 1315–1330, http://dx.doi.org/10.1016/j.physa.2019.04.122.
[7] S. Pahwa, A. Hodges, C. Scoglio, S. Wood, Topological analysis of the power grid and mitigation strategies against cascading failures, in: 2010 IEEE International Systems Conference, 2010, pp. 272–276, http://dx.doi.org/10.1109/SYSTEMS.2010.5482329.
[8] S. Pahwa, C. Scoglio, A. Scala, Abruptness of cascade failures in power grids, Sci. Rep. 4 (2014) 3694, http://dx.doi.org/10.1038/srep03694.
[9] S.V. Buldyrev, R. Parshani, G. Paul, H.E. Stanley, S. Havlin, Catastrophic cascade of failures in interdependent networks, Nature 464 (2010) 1025–1028, http://dx.doi.org/10.1038/nature08932.
[10] X. Li, H. Wu, C. Scoglio, D. Gruenbacher, Robust allocation of weighted dependency links in cyber–physical networks, Physica A 433 (2015) 316–327, http://dx.doi.org/10.1016/j.physa.2015.04.006.
[11] Q. Yang, D. Gruenbacher, J.L. Heier Stamm, G.L. Brase, S.A. DeLoach, D.E. Amrine, C. Scoglio, Developing an agent-based model to simulate the beef cattle production and transportation in southwest kansas, Physica A 526 (2019) 120856, http://dx.doi.org/10.1016/j.physa.2019.04.092.
[12] J. Zhong, F. Zhang, S. Yang, D. Li, Restoration of interdependent network against cascading overload failure, Physica A 514 (2019) 884–891, http://dx.doi.org/10.1016/j.physa.2018.09.130.
[13] Z. Zhao, P. Zhang, H. Yang, Cascading failures in interconnected networks with dynamical redistribution of loads, Physica A 433 (2015) 204–210, http://dx.doi.org/10.1016/j.physa.2015.03.030.
[14] C.E. La Rocca, H.E. Stanley, L.A. Braunstein, Strategy for stopping failure cascades in interdependent networks, Physica A 508 (2018) 577–583, http://dx.doi.org/10.1016/j.physa.2018.05.154.
[15] Y. Shen, G. Ren, N. Zhang, G. Song, Q. Wang, B. Ran, Effects of mutual traffic redistribution on robustness of interdependent networks to cascading failures under fluctuant load, Physica A 560 (2020) 125138, http://dx.doi.org/10.1016/j.physa.2020.125138.
[16] M. Turalska, K. Burghardt, M. Rohden, A. Swami, R.M. D'Souza, Cascading failures in scale-free interdependent networks, Phys. Rev. E 99 (2019) 032308, http://dx.doi.org/10.1103/PhysRevE.99.032308.
[17] T. Zhang, Y. Zhang, X. Zhu, J. Chen, Cascading failures on interdependent networks with star dependent links, Physica A 535 (2019) 122222, http://dx.doi.org/10.1016/j.physa.2019.122222.
[18] C. Bode, S.M. Wagner, Structural drivers of upstream supply chain complexity and the frequency of supply chain disruptions, J. Oper. Manag. 36 (2015) 215–228, http://dx.doi.org/10.1016/j.jom.2014.12.004.
[19] D. Ivanov, B. Sokolov, A. Dolgui, The ripple effect in supply chains: trade-off 'efficiency-flexibility-resilience' in disruption management, Int. J. Prod. Res. 52 (2014) 2154–2172, http://dx.doi.org/10.1080/00207543.2013.858836.
[20] R. Reyes Levalle, S.Y. Nof, Resilience by teaming in supply network formation and re-configuration, Int. J. Prod. Econ. 160 (2015) 80–93, http://dx.doi.org/10.1016/j.ijpe.2014.09.036.
[21] S. Hosseini, N. Morshedlou, D. Ivanov, M.D. Sarder, K. Barker, A.A. Khaled, Resilient supplier selection and optimal order allocation under disruption risks, Int. J. Prod. Econ. 213 (2019) 124–137, http://dx.doi.org/10.1016/j.ijpe.2019.03.018.
[22] B. Canis, Motor Vehicle Supply Chain: Effects of the Japanese Earthquake and Tsunami, DIANE Publishing, 2011.
[23] Y. Zeng, R. Xiao, Modelling of cluster supply network with cascading failure spread and its vulnerability analysis, Int. J. Prod. Res. 52 (2014) 6938–6953, http://dx.doi.org/10.1080/00207543.2014.917769.

[24] L. Tang, K. Jing, J. He, H.E. Stanley, Complex interdependent supply chain networks: Cascading failure and robustness, Physica A 443 (2016) 58–69, http://dx.doi.org/10.1016/j.physa.2015.09.082.
[25] Y. Zeng, R. Xiao, X. Li, A resilience approach to symbiosis networks of ecoindustrial parks based on cascading failure model, Math. Probl. Eng. 2013 (2013) e372368, http://dx.doi.org/10.1155/2013/372368.
[26] Y. Wang, R. Xiao, An ant colony based resilience approach to cascading failures in cluster supply network, Physica A 462 (2016) 150–166, http://dx.doi.org/10.1016/j.physa.2016.06.058.
[27] Y. Wang, F. Zhang, Modeling and analysis of under-load-based cascading failures in supply chain networks, Nonlinear Dynam. 92 (2018) 1403–1417, http://dx.doi.org/10.1007/s11071-018-4135-z.
[28] L. Tang, K. Jing, J. He, H.E. Stanley, Robustness of assembly supply chain networks by considering risk propagation and cascading failure, Physica A 459 (2016) 129–139, http://dx.doi.org/10.1016/j.physa.2016.04.030.
[29] J. Sun, J. Tang, W. Fu, Z. Chen, Y. Niu, Construction of a multi-echelon supply chain complex network evolution model and robustness analysis of cascading failure, Comput. Ind. Eng. 144 (2020) 106457, http://dx.doi.org/10.1016/j.cie.2020.106457.
[30] L. Huo, H. Guo, Y. Cheng, X. Xie, A new model for supply chain risk propagation considering herd mentality and risk preference under warning information on multiplex networks, Physica A 545 (2020) 123506, http://dx.doi.org/10.1016/j.physa.2019.123506.
[31] L. Geng, R. Xiao, Outer synchronization and parameter identification approach to the resilient recovery of supply network with uncertainty, Physica A 482 (2017) 407–421, http://dx.doi.org/10.1016/j.physa.2017.04.025.
[32] N. Goldbeck, P. Angeloudis, W. Ochieng, Optimal supply chain resilience with consideration of failure propagation and repair logistics, Transp. Res. E 133 (2020) 101830, http://dx.doi.org/10.1016/j.tre.2019.101830.
[33] J. Drzymalski, N.G. Odrey, G.R. Wilson, Aggregating performance measures of a multi-echelon supply chain using the analytical network and analytical hierarchy process, Int. J. Serv. Econ. Manag. 2 (2010) 286–306, http://dx.doi.org/10.1504/IJSEM.2010.033368.
[34] D. Ivanov, B. Sokolov, J. Kaeschel, A multi-structural framework for adaptive supply chain planning and operations control with structure dynamics considerations, European J. Oper. Res. 200 (2010) 409–420, http://dx.doi.org/10.1016/j.ejor.2009.01.002.
[35] H. Fang, D. Jiang, T. Yang, L. Fang, J. Yang, W. Li, J. Zhao, Network evolution model for supply chain with manufactures as the core, PLoS One 13 (2018) e0191180, http://dx.doi.org/10.1371/journal.pone.0191180.
[36] S. Zapperi, P. Ray, H.E. Stanley, A. Vespignani, First-order transition in the breakdown of disordered media, Phys. Rev. Lett. 78 (1997) 1408–1411, http://dx.doi.org/10.1103/PhysRevLett.78.1408.
[37] Y. Zhang, O. Yağan, Optimizing the robustness of electrical power systems against cascading failures, Sci. Rep. 6 (2016) 27625, http://dx.doi.org/10.1038/srep27625.
[38] J.M. Hernández, C. Pedroza-Gutiérrez, Estimating the influence of the network topology on the agility of food supply chains, PLoS One 14 (2019) e0218958, http://dx.doi.org/10.1371/journal.pone.0218958.
[39] S.R. Cardoso, A. Paula Barbosa-Póvoa, S. Relvas, A.Q. Novais, Resilience metrics in the assessment of complex supply-chains performance operating under demand uncertainty, Omega 56 (2015) 53–73, http://dx.doi.org/10.1016/j.omega.2015.03.008.
[40] O. Yağan, Robustness of power systems under a democratic-fiber-bundle-like model, Phys. Rev. E 91 (2015) 062811, http://dx.doi.org/10.1103/PhysRevE.91.062811.
[41] A. Scala, P.G. De Sanctis Lucentini, The equal load-sharing model of cascade failures in power grids, Physica A 462 (2016) 737–742, http://dx.doi.org/10.1016/j.physa.2016.06.034.
[42] Daniels Henry Ellis, Jeffreys Harold, The statistical theory of the strength of bundles of threads. I, Proc. R. Soc. Lond. Ser. A 183 (1945) 405–435, http://dx.doi.org/10.1098/rspa.1945.0011.